COMPUTATION OF LFT UNCERTAINTY BOUNDS WITH REPEATED PARAMETRIC UNCERTAINTIES

K. B. Lim*, D. P. Giesy†
NASA Langley Research Center, MS 161, Hampton, Virginia, 23681-0001

Abstract

A new methodology in which linear fractional transformation uncertainty bounds are directly constructed for use in robust control design and analysis is proposed. Existence conditions for model validating solutions with or without repeated scalar uncertainty are given. The approach is based on minimax formulation to deal with multiple non-repeated structured uncertainty components subject to fixed levels of repeated scalar uncertainties. Input directional dependence and variations with different experiments are addressed by maximizing uncertainty levels over multiple experimental data sets. Preliminary results show that reasonable uncertainty bounds on structured non-repeated uncertainties can be identified directly from measurement data by assuming reasonable levels of repeated scalar uncertainties.

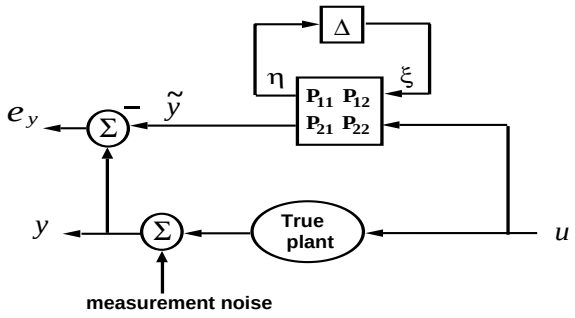

Figure 1: Block diagram for uncertainty identification

1 Problem Definition

Figure 1 shows measured input, $u \in \mathcal{C}^{n_u}$ and output, $y \in \mathcal{C}^{n_y}$, across a true plant. These inputs and outputs are assumed to be discrete Fourier transforms obtained from discrete time records. The corresponding output, $\tilde{y}$, from an upper linear fractional transformation model, $F_u(P, \Delta)$, depends on a given augmented plant, P, and an assumed structured uncertainty of the form

$$\Delta = \text{blk–diag}(\Delta_1, \ldots, \Delta_\tau);\ \Delta_i \in C^{m_i \times n_i},\ i \in T_\tau \qquad (1)$$

where $T_\tau := (1, \ldots, \tau)$. Consider a set of measurements from n_e independent experiments whose inputs and outputs are denoted by $(u^{(j)}, y^{(j)})$ for the jth experiment. Define the set

$$T_{n_e} := \{u^{(j)}, y^{(j)} : j = 1, \ldots, n_e\} \qquad (2)$$

Henceforth, consider input and output pairs that satisfy $(u, y) \in T_{n_e}$. At each frequency, the signals ξ and η depend on input vector u and in particular its direction so that a ratio of their norms will also be dependent on the particular input direction. To account for this dependence, consider satisfying model validating conditions [1] - [5] for all available experiments:

$$\xi = \Delta\eta \qquad (3)$$

$$\eta = P_{11}\xi + P_{12}u \qquad (4)$$

$$e_y = y - P_{21}\xi - P_{22}u = 0,\ \forall (u, y) \in T_{n_e} \qquad (5)$$

The basic problem we address is to determine smallest bounds among all uncertainties which are model validating with respect to available input/output measurements. From equation (3), the uncertainty bound can be written as a ratio of 2-norms

$$\frac{\|\xi\|_2}{\|\eta\|_2} \le \sup_{\eta'} \frac{\|\xi'\|_2}{\|\eta'\|_2} = \sup_{\eta'} \frac{\|\Delta\eta'\|_2}{\|\eta'\|_2} := \bar{\sigma}(\Delta) \qquad (6)$$

Of course fictitious signals ξ and η cannot be measured so it is necessary to look at their dependence on real signals u and y and their transmission through the system P. We consider a constant matrix problem; i.e., the supremum is taken at each frequency and is due to the directional dependence of ratio of 2-norms.

Let $\text{col}(\xi_1, \cdots, \xi_\tau)$ and $\text{col}(\eta_1, \cdots, \eta_\tau)$ be the partitioning of the vectors ξ and η which conform to the block diagonal partition of Δ in equation (1). For convenience, assume that all repeated scalar blocks are grouped into the first r blocks in Δ. Then, equation (3) becomes:

$$\begin{Bmatrix} \xi_1 \\ \vdots \\ \xi_r \\ \xi_{r+1} \\ \vdots \\ \xi_\tau \end{Bmatrix} = \text{blk-diag}(\Phi, \Delta_{r+1}, \ldots, \Delta_\tau) \begin{Bmatrix} \eta_1 \\ \vdots \\ \eta_r \\ \eta_{r+1} \\ \vdots \\ \eta_\tau \end{Bmatrix} \qquad (7)$$

where $\Phi := \text{blk-diag}(\delta_1 I_{n_1}, \ldots, \delta_r I_{n_r})$, and $\delta_i \in \mathcal{F}$ and Δ_i are defined in equation (1).

Given a model validating set, consider choosing a "smallest" size uncertainty in terms of

$$\bar{\sigma}(\Delta) = \max_{i \in T_\tau} \bar{\sigma}(\Delta_i), \qquad (8)$$

i.e., minimum over maximum over all components. A potential hazard with this viewpoint is the numerical values of the component uncertainties may not be of equal physical relevance. This is particularly true for more complex systems where there is usually a mixture of parametric (repeated or not) and nonparametric uncertainties including unmodeled dynamics. In practice, more uncertainty parameters are used (as compared to the "true" set of uncertain parameters) to sufficiently satisfy existence of model validating solutions. This means that robust identification problems generally lead to underdetermined problems, which appears to require the selection of physically significant uncertainty configurations and levels from all model validating sets. For the above reasons, we treat the parametric scalar uncertainties which

*Research Engineer, Guidance & Control Branch, Flight Dynamics & Control Division, k.b.lim@larc.nasa.gov

†Mathematician, Guidance & Control Branch, Flight Dynamics & Control Division, d.p.giesy@larc.nasa.gov

are often repeated separately from component unstructured uncertainties.

2 Existence of ξ, η

For each experiment, consider the existence of ξ which is an unconstrained by the structure in the uncertainty block and satisfying equation (5) which is rewritten as

$$P_{21}\xi = y - P_{22}u := e_y^o,\ (u,y) \in T_{n_e} \tag{9}$$

Lemma 1: For each $(u,y) \in T_{n_e}$, a ξ exists which satisfies equation (5) if and only if

$$e_y^o \in \mathrm{Im}(P_{21}) \quad \square \tag{10}$$

Lemma 1 is a test which gives a yes or no answer. If the test indicates that a solution exists, then all ξ satisfying equation (5) can be written as

$$\xi = P_{21}^{+} e_y^o + N_{21}\psi \tag{11}$$

where e_y^o is determined by the particular experiment using equation (9), N_{21} is chosen so that its columns span $\mathrm{Ker}(P_{21})$, and $\psi \in \mathcal{C}^{n_\psi}$ is arbitrary. Given any ξ from equation (11), the complementary signal η can be computed from equation (4).

Lemma 1 defines the conditions under which the output nominal error e_y^o can be cancelled by the fictitious signals $P_{21}\xi$ from the uncertainty block. The Lemma presupposes that the fictitious signal ξ is unconstrained by the structure in the uncertainty block. Note that the null freedom ψ is an independent variable. In fact, any choice of ψ for a given experiment gives a corresponding pair of ξ and η which satisfy equations (4) and (5).

If the condition in Lemma 1 holds, the fictitious signals satisfying equations (4) and (5) can be written as

$$\begin{Bmatrix} \eta \\ \xi \end{Bmatrix} = \begin{Bmatrix} b \\ a \end{Bmatrix} + \begin{bmatrix} P_{11} \\ I \end{bmatrix} N_{21}\psi \tag{12}$$

where

$$b := P_{11}P_{21}^{+}e_y^o + P_{12}u \tag{13}$$

$$a := P_{21}^{+}e_y^o \tag{14}$$

It turns out that for general complex block diagonal uncertainty structure with no repeated scalar blocks, for given ξ and η, a Δ satisfying equation (3) always exists [1]. Consequently we state the following result which was also obtained earlier in [4] in a more general context.

Theorem 1 (no repeated scalar block)
Let $(u,y) \in T_{n_e}$. Then a corresponding model validating uncertainty set, ξ, η, and Δ, satisfying equations (3) to (5) exists if and only if $e_y^o \in \mathrm{Im}(P_{21})$. $\square$

If Δ contains repeated scalar blocks, then the condition in Theorem 1 becomes only a necessary condition for model validation. So, with repeated scalar blocks we ask, "Among all pairs (ξ,η), satisfying equation (12), does a pair exist that also satisfies equation (3)?" Given any pair (ξ,η), Δ_{r+1}, ..., Δ_τ always exist, so we need to consider only the existence of the first r blocks, $\delta_1 I_{n_1}$, ..., $\delta_r I_{n_r}$. Let us denote $\bar{n} := \sum_{i=1}^{r} n_i = \bar{m} := \sum_{i=1}^{r} m_i$ and define

$$Z := \left[-\Phi, 0_{\bar{n}\times(n-\bar{n})}, I_{\bar{m}}, 0_{\bar{m}\times(m-\bar{m})}\right] \tag{15}$$

Theorem 2 (with repeated scalar block)
Suppose the condition in Theorem 1 holds. Let $(u,y) \in T_{n_e}$. Then, a model validating set ξ, η, and Δ exists if and only if there exists $\delta_1,\ldots,\delta_r$, and ψ such that

$$\begin{Bmatrix} b \\ a \end{Bmatrix} + \begin{bmatrix} P_{11} \\ I \end{bmatrix} N_{21}\psi \in \mathrm{Ker}(Z(\delta_1,\ldots,\delta_r)) \ \square \tag{16}$$

Theorem 2 is a constraint on ψ to limit ξ and η that satisfy the repeated scalar structure implicit in equation (7). Note that Z has full row rank independent of the set $\delta_1,\ldots,\delta_r$, so that

$$\dim(\mathrm{Ker}(Z)) = n + m - \bar{n} \tag{17}$$

Note that although the rank of Z does not change as long as $\delta_i \neq 0, \forall i \in T_r$, the bases changes with δ_i, $i \in T_r$, due to the repeated scalar uncertainty structure. Theorem 2 results in either a yes or no answer to the existence question. However, as a test, it is complicated because Z is dependent on the values of the set $\delta_1,\ldots,\delta_r$, which is as yet undetermined.

3 Uncertainty Bound

3.1 Uncertainty Bound Inequality

From equation (8), it is of interest to note that

$$\frac{\|\xi_i\|_2}{\|\eta_i\|_2} \leq \sup_{\eta_i'} \frac{\|\xi_i'\|_2}{\|\eta_i'\|_2} = \sup_{\eta_i'} \frac{\|\Delta_i\eta_i'\|_2}{\|\eta_i'\|_2} := \bar{\sigma}(\Delta_i),\ i \in T_\tau \tag{18}$$

With physical signals, the best we can expect to do is to estimate the supremum by a maximum over all available experiments, i.e.,

$$\bar{\sigma}(\Delta_i) \approx \max_{(u,y)\in T_{n_e}} \frac{\|\xi_i\|_2}{\|\eta_i\|_2} := \max_{(u,y)\in T_{n_e}} \delta_i := \bar{\delta}_i,\ i \in T_\tau \tag{19}$$

For each experiment, the free null parameter ψ (and therefore ξ and η) can be chosen that minimizes the ratio of 2-norms in equation (19). The maximum over all experiments in equation (19) can be determined after solving for minimum ratio with respect to ψ for each experiment, independently. Hence, consider first the following minimization problem for each experiment:

$$\min_{\psi} \frac{\|\xi_i(\psi)\|_2}{\|\eta_i(\psi)\|_2} := \delta_{i*} \quad i \in T_\tau \tag{20}$$

The asterisk in equation 20 refers to the minimum 2-norm ratio with respect to ψ. To avoid a ratio of square root of quadratics in ψ, consider the condition

$$J_i := \|\xi_i(\psi)\|_2^2 - \delta_i^2\|\eta_i(\psi)\|_2^2 \leq 0, \quad i \in T_\tau \tag{21}$$

Notice that δ_{i*} in equation (20) is the smallest δ_i making equation (21) true for all ψ. A violation of inequality (21) implies that δ_i is not an upper bound on the ratio of signal norms, i.e., it fails as an uncertainty bound. For large δ_i, equation (21) is more likely to be satisfied, which makes intuitive sense. Finally, notice that in equation (20), ψ generally influences all components ξ_i, η_i, $i \in T_\tau$. This motivates the minimax formulation.

3.2 Minimax problem

The problem for each experiment then becomes: find the smallest bound set, $\bar{\delta}_{i*}$, $i \in T_\tau$, such that inequality (21) is satisfied and subject to model validation constraints on ξ_i and

η_i. The signal ψ is a free parameter from excess uncertainty degrees of freedom that can be judiciously chosen for each experiment to minimize J_i for all i. The multiple objective nature is addressed by formulating it as a particular type of minimax problem.

Using Theorem 2, we can parameterize the set of all signal pairs, (ξ, η) that satisfies model validation for each experiment. This set corresponds to all ψ, and $\delta_1,\ldots,\delta_r$ that satisfies equation (16) which can be rewritten as

$$(-\Phi P_{11_{\bar{n}}} + N_{21_{\bar{n}}})\psi = \Phi b_{\bar{n}} - a_{\bar{n}} \tag{22}$$

and $(\cdot)_{\bar{n}}$ denotes the first $\bar{n}$ rows of $(\cdot)$. Notice from equation (22) that it depends only on the repeated scalar uncertainties.

In our approach, we choose to restrict a model validating set parameterized by the set ψ, and $\delta_1,\ldots,\delta_r$ that is also bounded by

$$|\delta_i| \le \bar{\delta}_i, \quad i = 1,\ldots,r \tag{23}$$

where $\bar{\delta}_i \in R$ which denotes the ith repeated scalar uncertainty bound as chosen a priori by an engineer. With the remaining freedom in the restricted model validating set, we seek a smallest uncertainty bound for the remaining nonrepeated uncertainty components $(i = r+1,\ldots,\tau)$.

We summarize the problem for each experiment as

$$\underline{\textbf{OP1}} \qquad \min_{\delta_1,\ldots,\delta_r,\psi} \left(\max_{i=r+1,\ldots,\tau} \{\bar{\delta}_i^2\} \right)$$

subject to equations (22), (23), and

$$\begin{aligned} -\bar{\delta}_i^2 \|b_{n_i} + P_{11_{n_i}} N_{21}\psi\|_2^2 &+ \|a_{m_i} + N_{21_{m_i}}\psi\|_2^2 \le 0, \\ i &= r+1,\ldots,\tau \end{aligned}$$

where $(\cdot)_{n_i}$ and $(\cdot)_{m_i}$ refers to the ith block of rows associated with $\Delta_i \in C^{m_i \times n_i}$ of dimensions n_i and m_i respectively for matrix $(\cdot)$. The possible non-smoothness in the minimax problem in OP1 can be avoided by recasting the problem for each experiment as

$$\underline{\textbf{OP2}} \qquad \min_{\delta_1,\ldots,\delta_r,\bar{\delta}_{r+1}^2,\ldots,\bar{\delta}_\tau^2,\psi,\gamma} \gamma \tag{24}$$

subject to equations 22,23, and

$$\begin{aligned} -\bar{\delta}_i^2 \|b_{n_i} + P_{11_{n_i}} N_{21}\psi\|_2^2 &+ \|a_{m_i} + N_{21_{m_i}}\psi\|_2^2 \le 0, \\ i &= r+1,\ldots,\tau \end{aligned} \tag{25}$$

$$\bar{\delta}_i^2 - \gamma \le 0, \quad i = r+1,\ldots,\tau \tag{26}$$

The dimensions of the equations are as follows: equation (22) consists of $\bar{n}$ complex equalities, equation (23) consists of r real inequalities, equation (25) consists of $\tau - r$ real inequalities, and equation (26) consists of $\tau - r$ real inequalities. Equation (22) defines the admissible set of fictitious signals parameterized by ψ that satisfies the repeated scalar uncertainty structure. Equation (25) defines the dependence of nonrepeated uncertainty bounds on the above admissible set of fictitious signals. Finally, condition (23) specifies the bound on repeated scalar uncertainties while condition (26) is used to define a bound on the maximum nonrepeated uncertainty component for minimax optimization purpose.

3.3 No repeated scalar block

For the case when there are no repeated scalar blocks $(r = 0)$, OP2 reduces to

$$\min_{\bar{\delta}_1^2,\ldots,\bar{\delta}_\tau^2,\psi,\gamma} \gamma \quad \text{subject to conditions (25) and (26).}$$

Note from condition (25) that for any fixed ψ, the smallest $\bar{\delta}_i^2$ holds when condition (25) becomes an equality, i.e.,

$$\bar{\delta}_i^2 = \frac{\|a_{m_i} + N_{21_{m_i}}\psi\|_2^2}{\|b_{n_i} + P_{11_{n_i}} N_{21}\psi\|_2^2}, \quad i \in T_\tau \tag{27}$$

The OP2 problem for each experiment reduces to the following:

$$\underline{\textbf{OP3}} \qquad \min_{\psi,\gamma} \gamma \tag{28}$$

subject to

$$\bar{\delta}_i^2 = \frac{\|a_{m_i} + N_{21_{m_i}}\psi\|_2^2}{\|b_{n_i} + P_{11_{n_i}} N_{21}\psi\|_2^2} \le \gamma, \quad i \in T_\tau \tag{29}$$

In OP3, the null freedom vector ψ is used to minimize the maximum uncertainty bound. Note that for each experiment (or $n_e = 1$ case), OP3 is equivalent to the earlier results using a minimum norm model validating (MNMV) formulation as given in [1]-[2].

3.4 Compuational Algorithm

For numerical solutions, we suggest the following steps:

Step 1: Choose repeated scalar bounds $\bar{\delta}_i$, $i = 1,\ldots,r$.

Step 2: Solve optimization problem OP2 for each experiment.

If OP2 results in an infeasible domain, increase appropriate $\bar{\delta}_i$. Redo Step 2 until solution exists.

Step 3: Compute worst bounds for nonrepeated uncertainty components over all experiments.

$$\bar{\delta}_i = \max_{T_{n_e}} \bar{\delta}_{i*}, \quad i = r+1,\ldots,\tau$$

Step 4: Fit uncertainty components using stable low order rational functions over all frequencies.

Note that in Step 4, an interactive utility program such as `drawmag`, a μ-Tools command [6] can be used. Analytical sensitivities for all constraint functions are derived and used but not shown due to lack of space. All complex variables and equations are expanded out in real variable form to obtain the derivatives.

4 Illustrative Example

Consider a simple dyamical system given in [5] but with two force inputs and two outputs. The system consists of two structural modes resulting in four state variables. The system is discretized at 50 Hertz assuming a zero order hold at both inputs. The fourth order discrete A matrix for this system has the form

$$A = \text{blk-diag}(A_1, A_2) \tag{30}$$

where A_i is a 2 by 2 matrix of the form

$$A_i := \begin{bmatrix} \text{Re}(z_i) & -\text{Im}(z_i) \\ \text{Im}(z_i) & \text{Re}(z_i) \end{bmatrix} \tag{31}$$

To establish a truth model which is then used to simulate measurements, we perturb the first structural mode by the following

$$A_1 = A_1^o + \delta_1 \begin{bmatrix} 1 & 0 \\ 0 & 1 \end{bmatrix} + \delta_2 \begin{bmatrix} 0 & -1 \\ 1 & 0 \end{bmatrix} \tag{32}$$

where δ_1 and δ_2 corresponds to the perturbations in the real and imaginary components of the first discrete eigenvalue, respectively. The perturbation matrices for this choice of parametric uncertainties are of rank two, i.e., repeated multiplicity of order 2 for each scalar parameter. Of course in order to preserve the complex conjugate pair property of the set of perturbed plants, both δ_1 and δ_2 must be real numbers. For the simulated measurements, a small level of independent Gaussian white noise was included at both outputs. A single time record was divided into two segments for use as two independent experiments ($n_e = 2$).

4.1 Nominal and Uncertainty Structure

Consider a nominal model consisting of only the first mode with parametric perturbations set to $\delta_1 = \delta_2 = 0$. Hence, the nominal model contains both parametric error (in the first mode) and unmodeled dynamics (truncated second mode). Figure 2 shows the poles of the true plant corresponding to the two structural modes and an approximation of the first pole by the nominal model. This parametric error is represented

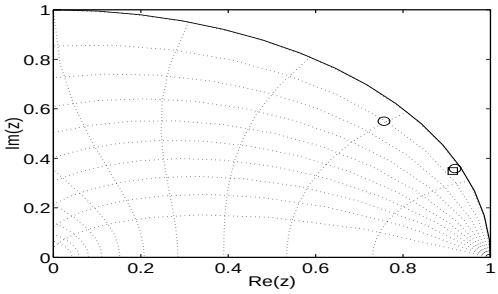

Figure 2: True($\circ$), nominal($\square$) poles.

in the state space form [7]

$$\begin{bmatrix} A & B \\ C & D \end{bmatrix} = \begin{bmatrix} A_o & B_o \\ C_o & D_o \end{bmatrix} + \sum_{i=1}^{2} \delta_i \begin{bmatrix} E_i \\ F_i \end{bmatrix} \begin{bmatrix} G_i & H_i \end{bmatrix} \quad (33)$$

where $E_1 = G_1 = G_2 = I_{2\times 2}$, $F_1 = H_1 = F_2 = H_2 = 0_{2\times 2}$, and $E_2 = [0, -1; 1, 0]$.

Figure 3 shows the interconnection structure of the parametric uncertainty with an additive uncertainty from two inputs to two outputs. Figure 4 shows the frequency

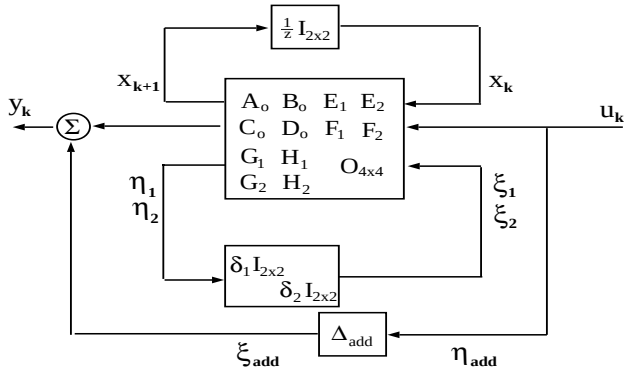

Figure 3: Nominal and uncertainty interconnection.

response of the true model, nominal, and a difference (true - nominal), from input 1 to both outputs. Notice that the difference between the nominal and true system (dot) is the most significant at the two structural resonant frequencies. The first error peak is due to parametric error in the first mode and the second due to truncated second mode.

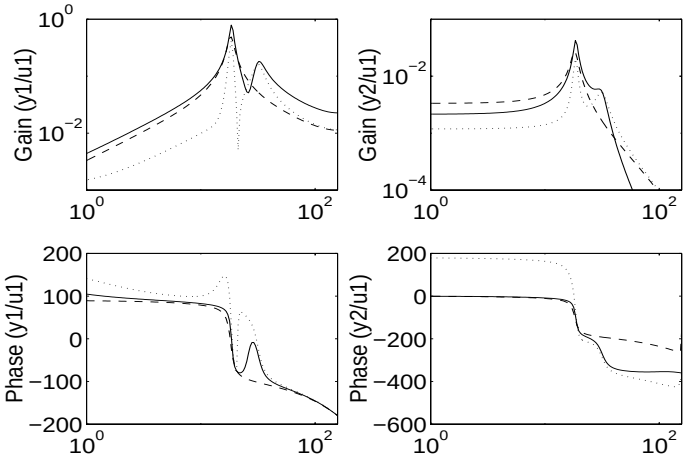

Figure 4: Frequency response of True($-$), Nominal($--$), and Additive error($\cdots$).

4.2 Parametric Study

Table 1 show the true and three different cases of assumed bounds of repeated scalar uncertainties. These three assumed sets of uncertainty bounds for the pair of repeated scalar uncertainties are used to compute the corresponding smallest additive uncertainties. Notice that Case 1 greatly underestimates the true values while Case 3 greatly overestimates it. On the other hand, Case 2 represents a level near the true parameter levels, i.e., a good guess. The optimization problem (OP2) for all three cases were solved using a Sequential Quadratic Programming algorithm found in MATLAB Optimization Toolbox [8].

Table 1: True and assumed parametric uncertainties.

	δ_1	δ_2
True	.005	.01
Case 1	.001	.001
Case 2	.01	.01
Case 3	.1	.1

4.3 Discussion of results

Figures 5 to 7 show the identified uncertainty bounds for unmodeled dynamics ($\circ$) while figure 8 shows the corresponding curved-fitted stable low order rational functions for additive uncertainties in all three cases. It appears that when the assumed parametric uncertainty bound is very small relative to true values (Case 1, figure 5), the additive uncertainty tries to capture a large error incurred by the optimistic level of assumed parametric uncertainty. When the assumed parametric uncertainty level is near true levels (Case 2, figure 6), the additive uncertainty show much smaller levels at frequencies where the parametric errors are expected to be significant. This reduction of the identified unmodeled dynamics at these frequencies is even more pronounced in Case 3 (figure 7) where the assumed parametric uncertainty level is more than an order of magnitude larger than true values.

In all three cases, the identified levels for the unmodeled dynamics is unchanged to a large extent. This observation

is consistent with the expectation that in general, parametric changes for a structural mode do not significantly affect other structural modes.

Finally, note that from a more detailed parametric study, a smaller level of parametric uncertainty level could be deduced. This "minimal" parametric uncertainty level corresponds to a threshold level whereby a further decrease in the parametric uncertainty level will give a large increase in unmodeled dynamics uncertainty level. Of course, a priori physical knowledge of the system under investigation will generally help in determining this optimal tradeoff point.

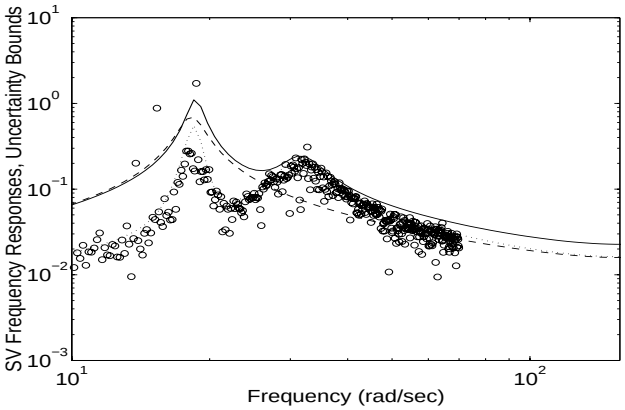

Figure 5: Case 1: Additive unc bounds ($\circ$) and SV frequency responses - True($-$), Nominal($--$), True-Nominal($\cdots$)

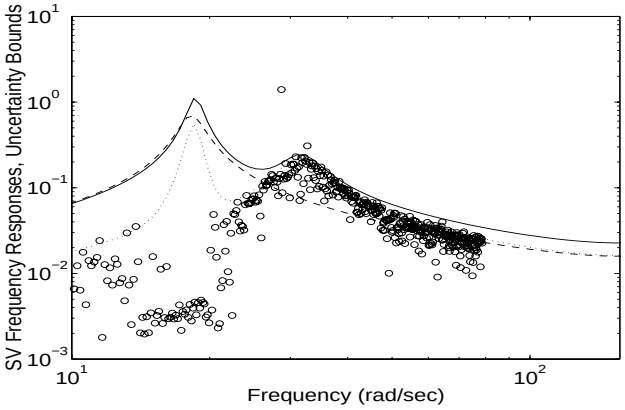

Figure 6: Case 2: Additive unc bounds ($\circ$) and SV frequency responses - True($-$), Nominal($--$), True-Nominal($\cdots$)

5 Conclusion

A new algorithm is presented for identifying both non parametric uncertainties and repeated scalar uncertainties. The algorithm uses a minimax search which is constrained to all fictitious input/output uncertainty signal sets that zero out output errors for a nominal model. This development extends an earlier method involving a minimum norm model validating approach.

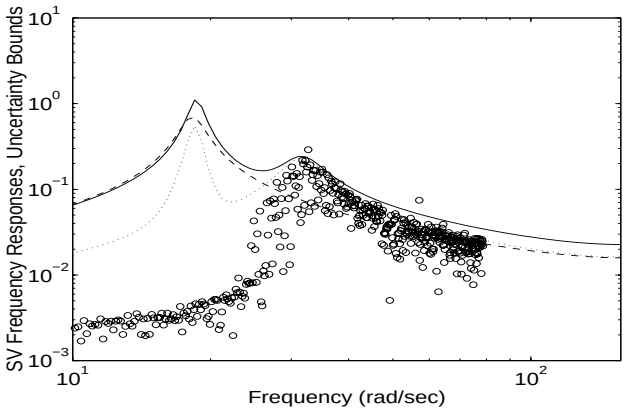

Figure 7: Case 3: Additive unc bounds ($\circ$) and SV frequency responses - True($-$), Nominal($--$), True-Nominal($\cdots$)

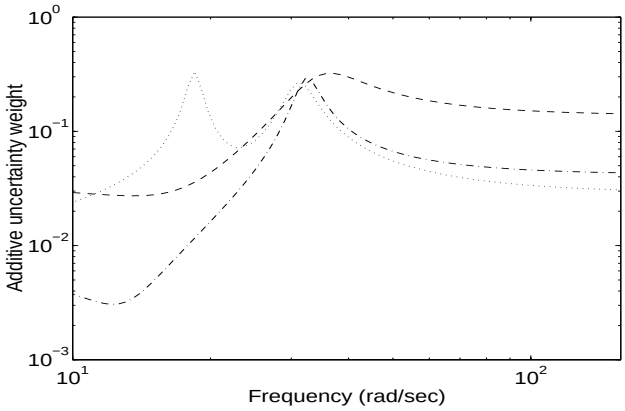

Figure 8: Fitted additive weighting function for Case 1 ($\cdots$), Case 2($--$), Case 3($-\cdot$)

References

[1] Lim, K.B., Balas, G.J., and Anthony, T.C., "Minimum-norm model validating identification for robust control," AIAA Paper No. 96-3717.

[2] Lim, K.B., "Closed form solution for minimum norm model validating uncertainty," *1997 American Control Conference*, Albuquerque, NM.

[3] Lim, K.B., Cox, D.E., Balas, G.J., and Juang, J-N., "Validation of an experimentally derived uncertainty model," *AIAA Journal of Guidance, Control, and Dynamics*, v.21, no.2, 1998.

[4] Smith, R.S., Doyle, J.C., "Model Validation: A connection between robust control and identification," *IEEE Transactions on Automatic Control*, vol 37, No 7, July 1992, pp.942-952.

[5] Kumar, A., and Balas, G.J., "A scaling approach to model validation in the μ framework," 1995 *American Control Conference*, pp.693-697.

[6] Balas, G.J., Doyle, J.C., Glover, K., Packard, A., and Smith, R., *μ-Analysis and Synthesis Toolbox*, MUSYN Inc., Minneapolis, MN, 1994.

[7] Morton, B., and McAfoos, R., "A Mu-test for real parameter variations," 1985 *American Control Conference*, Boston, MA.

[8] Branch, M.A., and A. Grace, *Optimization Toolbox*, The MathWorks, Inc., Natick, MA, December 1996.